ORGANIC CHEMISTRY
FRONTIERS

RESEARCH ARTICLE

View Article Online
View Journal | View Issue

Cite this: *Org. Chem. Front.*, 2014, **1**, 355

# Phenanthroline bridged bis(β-cyclodextrin)s/adamantane-carboxylic acid supramolecular complex as an efficient fluorescence sensor to $Zn^{2+}$†

Yu-Hui Zhang, Ying-Ming Zhang, Yong Chen, Yang Yang and Yu Liu*

Received 25th November 2013,
Accepted 18th February 2014

DOI: 10.1039/c3qo00054k

rsc.li/frontiers-organic

A water-soluble fluorescent $Zn^{2+}$ sensor, 1,10-phenanthroline bridged bis(β-cyclodextrin) (**1**), was synthesized by "click chemistry", and its fluorescence sensing behavior toward $Zn^{2+}$ against various metal ions was investigated under physiological conditions. Significantly, **1** showed high selectivity and sensitivity toward $Zn^{2+}$ with a limit of detection (LOD) down to $10^{-7}$ M. Moreover, the spectrophotometric studies demonstrated that after complexation with 1-admantanecarboxylic acid sodium salt (AdCA), the **1**/AdCA complex gave much stronger binding affinity and lower LOD value toward $Zn^{2+}$ through a cyclodextrin/substrate/$Zn^{2+}$ triple recognition mode. The fluorescence stopped-flow experiments also indicated that the association rate of complex **1**/AdCA to $Zn^{2+}$ was much faster than compound **1** to the same ion. Furthermore, the fluorescence intensity of **1** and **1**/AdCA was greatly enhanced after binding $Zn^{2+}$ in living cells, and thus **1** and complex **1**/AdCA could be considered as a biosensor for $Zn^{2+}$ at the cellular level.



## Introduction

The fluorescence sensing of $Zn^{2+}$ in water has drawn more and more attention in recent years, because $Zn^{2+}$ is closely related to our biomedical and physiological events.[1] As the second most abundant transition metal in the human body, $Zn^{2+}$ plays an important role in many kinds of biological processes, such as brain function and pathology, gene transcription, metalloenzyme regulation, immune function, and neural signal transmission.[2] Therefore, it is an increasingly significant topic to quantitatively detect $Zn^{2+}$ under physiological conditions. However, the zinc ion itself is spectroscopically silent due to its $3d^{10}4s^0$ electronic configuration, which seriously hinders the real-time monitoring of $Zn^{2+}$ in biological systems.[3] To solve this problem, a large number of fluorescent probes have been developed and exhibit excellent $Zn^{2+}$ responsiveness *in vitro* and *in vivo*, mainly due to their immense advantages of simplicity, high sensitivity and selectivity, instantaneous response, and local observation.[4] Nevertheless, among these fluorescent $Zn^{2+}$ chemosensors, only few of them are totally water-soluble and can detect $Zn^{2+}$ without disturbance from $Cd^{2+}$.[5]

Cyclodextrins (CDs), a class of cyclic oligosaccharides possessing a hydrophobic cavity, are widely used as drug carriers and solubilizers.[6] The modification of the CD backbone with chromophoric substituents has been proven as a more powerful strategy in the fluorescence sensing of transition- or heavy-metal ions. For instance, we have constructed a series of CD-based switch-on fluorescent sensors for $Zn^{2+}$, $Cd^{2+}$, and $Hg^{2+}$, showing satisfactory molecular selectivity and enhanced binding abilities in aqueous solution, thin film, and living cells.[7] In the present work, phenanthroline is connected with β-CD to obtain 1,10-phenanthroline bridged bis(β-CD) **1** by "click chemistry", which showed satisfactory water solubility and high fluorescence sensing efficiency for $Zn^{2+}$. The two adjacent CD cavities in **1** could not only act as an ideal solubilizer, but also endowed the phenanthroline core with cell permeability through the interaction of β-CD with the phospholipids and cholesterol on the cell membrane.[8] Moreover, due to the strong association of the β-CD cavity with the adamantyl skeleton, **1** could form a stable inclusion complex with 1-admantanecarboxylic acid sodium salt (AdCA), and the resultant **1**/AdCA complex exhibited much stronger binding ability, lower limit of detection (LOD) value, and faster reaction rate toward $Zn^{2+}$. Our obtained results will energize the potential use of CD-based bioactive nanosupramolecules in the construction of efficient fluorescence sensors with actual device implementation.

*Department of Chemistry, State Key Laboratory of Elemento-Organic Chemistry, Nankai University, Collaborative Innovation Center of Chemical Science and Engineering, Tianjin 300071, P. R. China. E-mail: yuliu@nankai.edu.cn*

†Electronic supplementary information (ESI) available: Experimental methods, synthetic routes and characterization of compounds **1** and **2**, Job plots of **1**/$Zn^{2+}$ and **1**/AdCA/$Zn^{2+}$ systems, the fluorescence changes ($\Delta F/F_0$) of **1** in the presence of different metal cations, as well as 2D NOESY spectra of **1**/AdCA/$Zn^{2+}$ system. See DOI: 10.1039/c3qo00054k

## Results and discussion

### Synthesis

The synthetic route to compound **1** is described in Scheme 1. Compound **1** was synthesized *via* "click chemistry" between 2,9-dipropargyl-1,10-phenanthroline and mono(6-deoxyl-6-azido)-β-CD[9] in 28% yield, and was sufficiently characterized by NMR spectroscopy, MALDI-MS, and elemental analysis (Fig. S1–S6 in the ESI†). Benefiting from the good solubilization ability of two adjacent β-CD units, the host compound **1** showed a satisfactory solubility up to 0.05 M in water.

### Fluorescence sensing of $Zn^{2+}$ by 1

The fluorescence sensing behavior of **1** toward $Zn^{2+}$ was investigated by means of fluorescence spectroscopy in HEPES buffer solution (10 mM, pH = 7.2) at 25 °C. As shown in Fig. 1, compound **1** showed a good fluorescence sensing ability for $Zn^{2+}$. The emission intensity of **1** at 377 nm gradually increased upon addition of $Zn^{2+}$, accompanied by an obvious bathochromic shift from 368 to 377 nm. Furthermore, a maximum peak at a molar fraction of 0.5 was clearly observed in the Job plot, corresponding to a 1 : 1 coordination stoichiometry between **1** and $Zn^{2+}$ (Fig. 2). After validating the 1 : 1 **1**/$Zn^{2+}$ stoichiometry, the binding constant (log $K_S$) between **1** and $Zn^{2+}$ could be calculated as 5.95 using a nonlinear least-squares curve-fitting method by analyzing the sequential changes in fluorescence intensity ($\Delta F$) of **1** in the presence of varying concentrations of $Zn^{2+}$.[10] In addition, the limit of detection (defined as LOD value) of **1** to $Zn^{2+}$ was measured as $4.92 \times 10^{-7}$ M by multiplying the standard derivation of 11 groups of blank measurements by 3 and then dividing by the slope of the linear calibration curve at the lower concentration range of $Zn^{2+}$.[11]

The possible mechanism for the enhanced fluorescence of **1**/$Zn^{2+}$ complex may originate from a controlled intramolecular photo-induced electron transfer (PET) process; that is, before coordination with $Zn^{2+}$, the PET process takes place from the 1,2,3-triazole moiety as an electron-rich donor to the phenanthroline moiety as an electron-deficient acceptor. After coordination with $Zn^{2+}$, the nonradiative channel in the PET process was synchronously suppressed to a great extent,

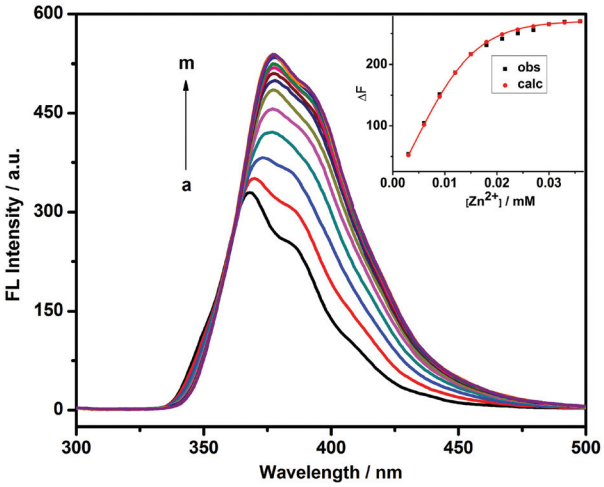


**Fig. 1** Fluorescence spectral changes of **1** ($1.5 \times 10^{-5}$ M) upon addition of $Zn(ClO_4)_2$ (0, 3, 6, 9, 12, 15, 18, 21, 24, 27, 30, 33, and $36 \times 10^{-6}$ M, from a to m) in HEPES buffer solution (10 mM, pH = 7.2). Inset: the nonlinear least-squares analysis of the differential fluorescence intensity ($\Delta F$) with the concentration of $Zn^{2+}$ to calculate the binding constant ($K_S$) ($\lambda_{ex}$ = 272 nm and $\lambda_{em}$ = 377 nm).

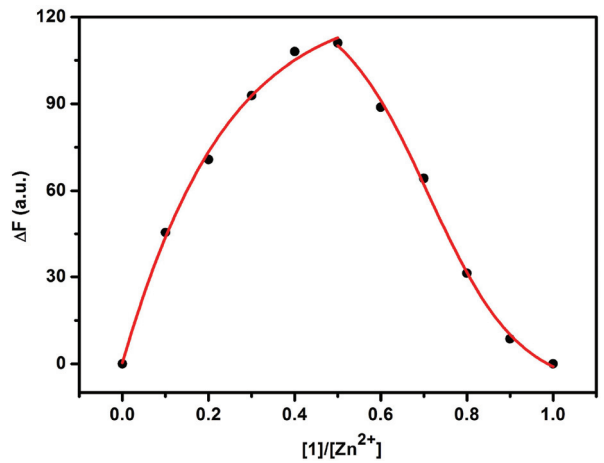


**Fig. 2** Job plot of **1**/$Zn^{2+}$ system in HEPES buffer solution (10 mM, pH = 7.2) at 25 °C ([**1**] + [$Zn^{2+}$] = $2.0 \times 10^{-5}$ M).

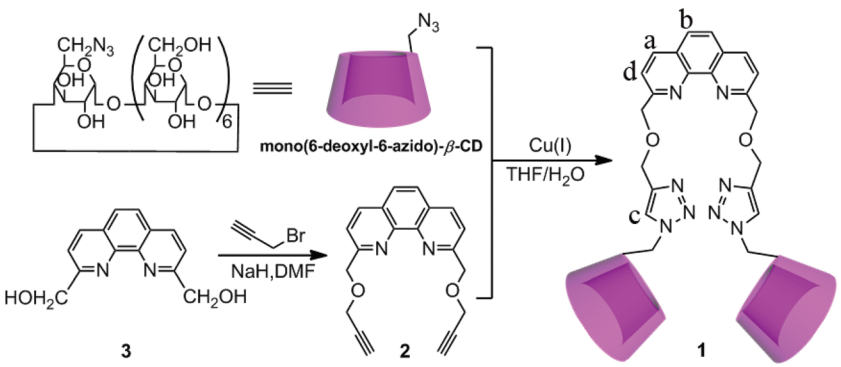


**Scheme 1** Synthetic route of compound **1**.

 

ultimately leading to a pronounced emission intensity of the phenanthroline fluorophore. Moreover, a favorable size/shape fit was achieved between the ionic radius of $Zn^{2+}$ and the semi-rigid structure of the phenanthroline and triazole units to form a five-membered chelating ring.

Comparatively, the fluorescence sensing selectivity of **1** toward various metal cations was also studied in a physiological environment. As shown in Fig. 3, the fluorescence of **1** showed a 2.1-fold fluorescence enhancement in the presence of 2 equiv. of $Zn^{2+}$, but its IIB homologue $Cd^{2+}$ only gave a negligible change under the same experimental conditions. Moreover, an obvious fluorescence quenching was observed when $Ag^{+}$, $Co^{2+}$, $Cu^{2+}$, $Hg^{2+}$, and $Pb^{2+}$ were added into the solution of **1**. These phenomena may be ascribable to the electron or energy transfer from the phenanthroline moiety of **1** to the unfilled electronic orbitals on these cations.

### Fluorescence sensing of 1/AdCA to $Zn^{2+}$

It is well-documented that there is a high affinity between the cavity of β-CD and adamantane derivatives with $K_S$ values up to $10^4$ $M^{-1}$. In the present work, 1-admantanecarboxylic acid sodium salt (AdCA) was employed to investigate the enhanced $Zn^{2+}$ binding stability and sensing ability of the **1**/AdCA inclusion complex (Fig. 4). In comparison to the fluorescence quenching with $Cd^{2+}$, it was found that the fluorescence intensity of **1**/AdCA was exclusively enhanced with $Zn^{2+}$ (Fig. S7†). Similar to the **1**/$Zn^{2+}$ system, the 1 : 1 coordination stoichiometry between **1**/AdCA and $Zn^{2+}$ was confirmed by a Job plot (Fig. S8†). Therefore, using the fluorescence titration method, the log $K_S$ value of **1**/AdCA with $Zn^{2+}$ was calculated as 7.74, which was almost 100 times higher than the corresponding value of **1** with $Zn^{2+}$. Meanwhile, a relatively lower LOD value was also obtained as $3.38 \times 10^{-7}$ M in **1**/AdCA to $Zn^{2+}$.

### Binding mode

The binding modes of **1** and **1**/AdCA with $Zn^{2+}$ were studied by means of $^1$H NMR, fluorescence spectroscopy, and circular dichroism spectroscopy. As shown in Fig. 5, the protons of the phenanthroline and triazole moieties of **1** exhibited a downfield shift ($\Delta\delta$) in the presence of $Zn^{2+}$ ($\Delta\delta_{a,1}$ = 0.37 ppm, $\Delta\delta_{b,1}$ = 0.04 ppm, $\Delta\delta_{c,1}$ = 0.29 ppm, and $\Delta\delta_{d,1}$ = 0.18 ppm), indicative of the electron deshielding effect of metal ions on the adjacent protons. Thus, we could deduce that the phenanthroline and triazole moieties of **1** participated in the coordination process with $Zn^{2+}$. Moreover, by employing a Hill plot,[11] the binding stoichiometry and log $K_S$ value between **1** and AdCA could be fitted as 2 and $4.2 \times 10^6$ $M^{-2}$, respectively, indicating that two AdCA units were concurrently encapsulated in the CD cavities to form a 2 : 1 complex with high affinity (Fig. S9 and S10 in the ESI†). Based on this binding constant, we can calculate that more than 90% of **1** was changed to the **1**/AdCA complex under our experimental conditions, and both CD cavities of **1** were occupied by AdCA to jointly coordinate with

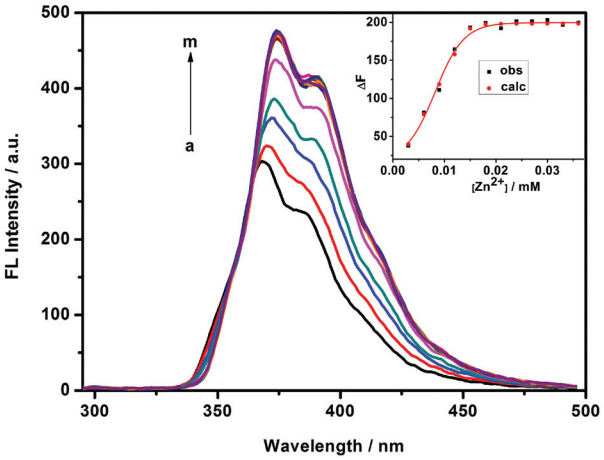


Fig. 4 Fluorescence emission spectra of **1** ($1.5 \times 10^{-5}$ M)/AdCA upon addition of $Zn(ClO_4)_2$ (0, 3, 6, 9, 12, 15, 18, 21, 24, 27, 30, 33, $36 \times 10^{-6}$ M from a to m) in HEPES buffer solution (10 mM, pH = 7.2). Inset: the non-linear least-squares analysis of the differential fluorescence intensity ($\Delta F$) with the concentration of $Zn^{2+}$ to calculate the complex binding constant ($K_S$) ($\lambda_{ex}$ = 272 nm, $\lambda_{em}$ = 377 nm).

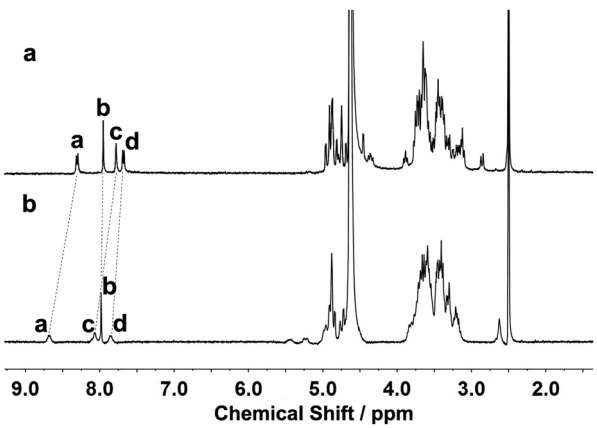


Fig. 5 $^1$H NMR spectra of (a) **1** and (b) **1**/$Zn^{2+}$ complex using DMSO as internal standard in $D_2O$ at 25 °C ([**1**] = $1.0 \times 10^{-3}$ M and [$Zn^{2+}$] = $2.0 \times 10^{-3}$ M).

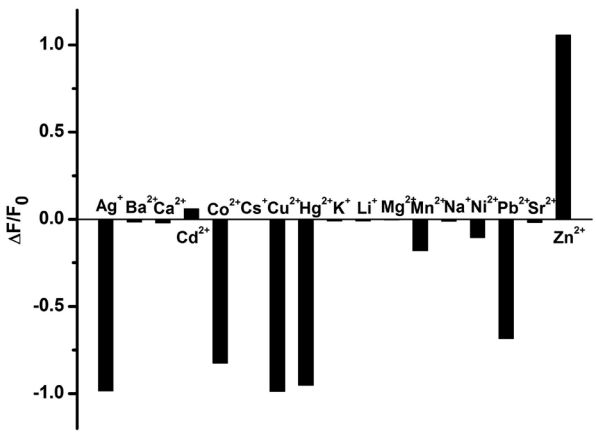


Fig. 3 Fluorescence change ($\Delta F/F_0$) of **1** at 377 nm in the presence of different metal cations in HEPES buffer (10 mM, pH = 7.2). ([**1**] = $1.5 \times 10^{-5}$ M, [$M^{n+}$] = $3.0 \times 10^{-5}$ M, $\lambda_{ex}$ = 272 nm).

$Zn^{2+}$. In addition, the fluorescence sensing of $Zn^{2+}$ was investigated with *ca.* 50% and 90% **1**/AdCA encapsulation ratios. As the AdCA encapsulation ratio increases, it is found that the fluorescence intensity of the **1**/AdCA/$Zn^{2+}$ ternary complex decreases accordingly (Fig. S11 in the ESI†). This result indicates that as compared with free host **1** and the 1 : 1 **1**/AdCA complex, the introduction of more AdCA can induce a slight fluorescent quenching in the coordination process.

Furthermore, 2D NMR spectroscopic experiments were performed to obtain structural information on the host–guest complexation. As shown in Fig. S12,† the nuclear Overhauser enhancement (NOE) cross-correlations between the protons of the 1,2,3-triazole ring and the H5 protons of the β-CD (peaks A), as well as those between the protons of the phenanthroline group and the H3 protons of the β-CD (peaks B and C), jointly demonstrate that the phenanthroline moiety of **1** was partially accommodated in the cavity of β-CD from its primary face. After adding 2 equiv. of $Zn^{2+}$, it was found that the phenanthroline spacer of **1** was still self-included in the cavity of β-CD (Fig. S13 in the ESI). In contrast, clear NOE correlations between the protons of AdCA and the interior protons of β-CD (H3/H5/H6) were observed (peaks A), and all the self-inclusion cross-peaks between phenanthroline and the CD cavity disappeared in the ternary complex of **1**/AdCA/$Zn^{2+}$ (Fig. S14 in the ESI†). In addition, the AdCA protons showed a stronger NOE correlation with H5/H6 than the H3 protons of β-CD. Considering that the H5/H6 protons are located near the narrow opening and the H3 protons are located near the wide opening of the β-CD cavity, we can infer that AdCA was preferentially located in the narrow opening and then drove the phenanthroline unit of **1** out of the cavity.

As shown in Fig. 6, the host **1** gave two induced circular dichroism (ICD) signals in aqueous solution. Based on the empirical rules for the ICD behavior of CD inclusion complexes,[12] the positive Cotton effect peak ($\Delta\varepsilon$ = 5.31 $M^{-1}$ $cm^{-1}$) at 230 nm and the negative one ($\Delta\varepsilon$ = −6.11 $M^{-1}$ $cm^{-1}$) at 272 nm reveal that the phenanthroline group is partially self-included in the chiral microenvironment of the β-CD cavity, which is in accordance with the intramolecular self-inclusion mode in the 2D NMR spectroscopic experiment. Moreover, it is found that the Cotton peak intensity of **1** slightly decreased in the presence of $Zn^{2+}$ or AdCA, mainly because the phenanthroline moiety was gradually released from the β-CD cavity. Conversely, when both $Zn^{2+}$ and AdCA coexisted, the ICD signals of **1** was reversed from a negative Cotton peak to a strong positive one, accompanied by enhanced signal intensity from $\Delta\varepsilon$ = −3.48 $M^{-1}$ $cm^{-1}$ to $\Delta\varepsilon$ = 27.89 $M^{-1}$ $cm^{-1}$ at 278 nm. These phenomena indicate that there is a conformational change upon complexation of **1** with $Zn^{2+}$ and AdCA. Due to the supramolecular cooperativity between CD and AdCA, the phenanthroline unit of **1** was forced out of the β-CD cavity to facilitate the multivalent binding of the phenanthroline, triazole, and carboxylic sites with $Zn^{2+}$.[13] Consequently, combining all the characteristic data from NMR and circular dichroism spectroscopy, we can reasonably deduce the possible binding modes of **1**/$Zn^{2+}$ and **1**/AdCA/$Zn^{2+}$, as illustrated in Scheme 2. In addition, the energy minimization structure of the **1**/AdCA/$Zn^{2+}$ system was obtained by a molecular modeling study, which is consistent with the proposed recognition mode (Fig. S15 in the ESI†).

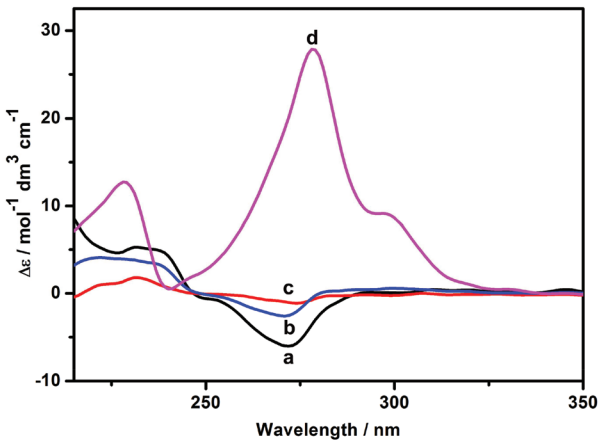


**Fig. 6** Circular dichroism spectra of (a) **1**, (b) **1**/AdCA complex, (c) **1**/$Zn^{2+}$ complex, and (d) **1**/AdCA/$Zn^{2+}$ complex in HEPES buffer solution at 25 °C ([**1**] = 1.5 × $10^{-5}$ M, [$Zn^{2+}$] = 3 × $10^{-5}$ M, and [AdCA] = 1 × $10^{-3}$ M).

### Binding dynamics

The binding dynamics for the association of **1** and **1**/AdCA with $Zn^{2+}$ were further measured by fluorescence stopped-flow experiments, in which the dynamic data can be simplified as a pseudo-first-order reaction in the presence of excess amounts of $Zn^{2+}$. The observed reaction rate constant ($k_{obs}$) could be determined by linear regression at different concentrations of $Zn^{2+}$.[14]

$$\mathbf{1} + Zn^{2+} \underset{k_{-}^{1}}{\overset{k_{+}^{1}}{\rightleftharpoons}} \mathbf{1}/Zn^{2+} \quad (1)$$

$$\mathbf{1}/\mathrm{AdCA} + Zn^{2+} \underset{k_{-}^{2}}{\overset{k_{+}^{2}}{\rightleftharpoons}} \mathbf{1}/\mathrm{AdCA}/Zn^{2+} \quad (2)$$

$$k_{obs} = k_{+}^{i}[Zn^{2+}] + k_{-}^{i} \quad (i = 1, 2) \quad (3)$$

where $k_{+}^{i}$ and $k_{-}^{i}$ are the rate constants for the forward and backward reactions for **1** and **1**/AdCA with $Zn^{2+}$, respectively. In the stopped-flow experiments, the values of $k_{+}^{1}$ and $k_{+}^{2}$ were measured as 3.94 × $10^{5}$ $M^{-1}$ $s^{-1}$ and 1.46 × $10^{6}$ $M^{-1}$ $s^{-1}$, respectively (Fig. 7 and Fig. S16†), indicating that the association rate of **1**/AdCA with $Zn^{2+}$ was much faster than that of **1** with $Zn^{2+}$. This is reasonable, because there are more binding sites in **1**/AdCA to accelerate the coordination of $Zn^{2+}$ in aqueous solution.

### Confocal fluorescent images *in vitro*

To gain more insight into the practical application of **1** and its corresponding supramolecular complex **1**/AdCA, the fluorescence sensing behaviors of **1** and **1**/AdCA toward $Zn^{2+}$ were studied *in vitro* by confocal fluorescent microscopy using HeLa human cervical carcinoma cells as the model cell line. As shown in Fig. 8a–c, the HeLa cells exhibited a weak blue fluo-

 

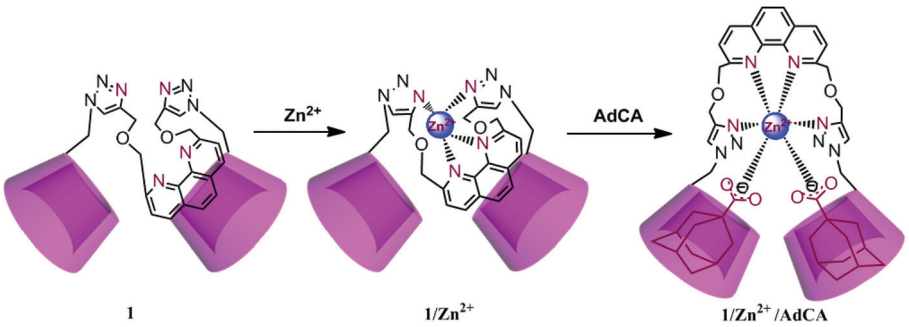


Scheme 2 The possible binding modes of **1**/$Zn^{2+}$ and **1**/AdCA/$Zn^{2+}$ systems.

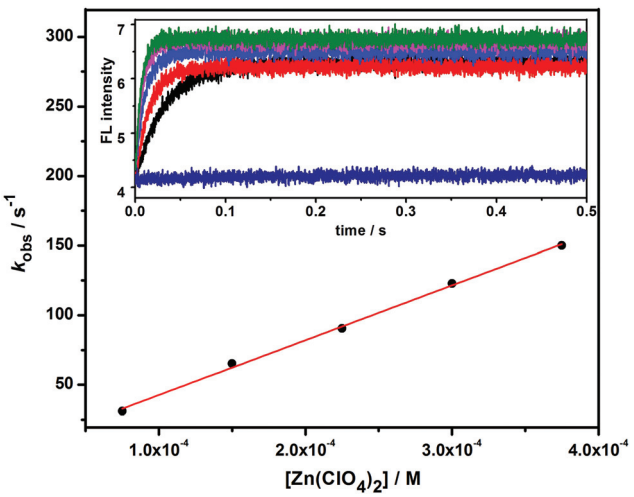


Fig. 7 Dependence of observed rate constant $k_{obs}$ of **1** ($1.5 \times 10^{-5}$ M) with different concentrations of $Zn^{2+}$ in HEPES buffer solution (10 mM, pH = 7.2). Inset: dynamic experiments of the rapid mixing of **1** ($1.5 \times 10^{-5}$ M) with different concentrations of $Zn(ClO_4)_2$ (0, 0.75, 1.5, 2.25, 3.0, and $3.75 \times 10^{-4}$ M). All concentrations mentioned above are final ones after mixing.

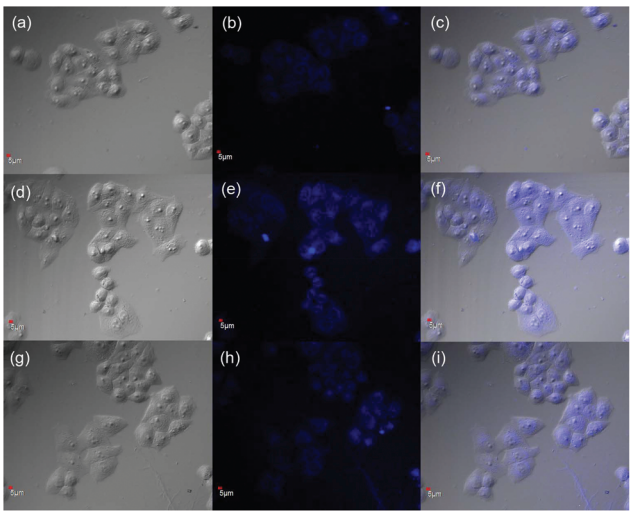


Fig. 8 Confocal fluorescence images of HeLa cells. (a)–(c) Cells incubated in the presence of **1** for 3 h; (d)–(f) cells pretreated with $Zn^{2+}$ for 0.5 h then incubated in the presence of **1** for 3 h; (g)–(i) cells pretreated with $Zn^{2+}$ for 0.5 h then incubated in the presence of **1** and AdCA for 3 h. (a), (d), and (g): Bright field images; (b), (e), and (h): fluorescence images; and (c), (f), and (i): merged images ([**1**] = $5 \times 10^{-5}$ M, [AdCA] = $5.7 \times 10^{-4}$ M, [$Zn^{2+}$] = $1 \times 10^{-4}$ M, and scale bar = 5 μm).

rescence after incubation with **1** alone at 37 °C for 3 h, but a strong blue fluorescence was observed when the same cells were pretreated with $Zn^{2+}$ for 0.5 h and then incubated with **1** for 3 h (Fig. 8d–f). A similar phenomenon was also observed in the case of **1**/AdCA/$Zn^{2+}$ system (Fig. 8g–i). These results indicate that, combined with their cell permeability and biocompatibility, **1** and **1**/AdCA could be used as the potential sensors for intracellular $Zn^{2+}$ detection.

## Conclusion

In conclusion, we successfully synthesized a water-soluble fluorescent $Zn^{2+}$ sensor **1** by "click chemistry". As investigated by fluorescent titration, it exhibited high selectivity and sensitivity toward $Zn^{2+}$ with a 1 : 1 binding mode. Study of the binding mode further revealed that the cooperative coordination of phenanthroline and triazole moieties played an indispensable role in the fluorescence sensing of $Zn^{2+}$. Superior to **1**, the **1**/AdCA system showed much stronger binding affinity, lower LOD value, and faster association rate toward $Zn^{2+}$ in aqueous solution. The confocal fluorescent images demonstrated that **1** and **1**/AdCA were cell-permeable and could effectively detect intracellular $Zn^{2+}$ at cellular level. Although the sensitivity toward $Zn^{2+}$ in the present work is moderate, the design strategy may act as a general and versatile platform to create an effective fluorescence $Zn^{2+}$ sensor with a longer emission wavelength. Considering the immense advantages in preparation, water solubility, and sensing specificity for $Zn^{2+}$, we also envision that the 1,10-phenanthroline bridged bis(β-CD) and its AdCA complex may have great application prospects in biological and environmental science and technology.

## Experimental section

### Synthesis of 1,10-phenanthroline bridged bis(β-CD) (1)

2,9-Bis(hydroxymethyl)-1,10-phenanthroline (90 mg, 0.285 mmol) in 10 mL THF was added to a solution of mono(6-deoxyl-

6-azido)-β-cyclodextrin (1.65 g, 1.42 mmol) in 35 mL water, then $CuSO_4 \cdot 5H_2O$ (710 mg, 2.84 mmol) and sodium ascorbate (1.4 g, 7.11 mmol) were added into the above solution. The mixture was heated at 50 °C under an atmosphere of $N_2$ for 2 days. The precipitate was filtered, and the filtrate was dried under reduced pressure. The residue was dissolved in a small amount of water, poured into 300 mL acetone and stirred, and then this process was repeated 3 times. Column chromatography using *n*-PrOH–$H_2O$–25% $NH_3 \cdot H_2O$ (6 : 3 : 2 v/v/v) as eluent yielded the crude product. Next, the crude product was further purified by MPLC (reversed phase) with water–ethanol (85 : 15 v/v) as eluent to give **1** as a pale yellow solid (240.7 mg, 28% yield). $^1$H NMR (400 MHz, $D_2O$, ppm): $\delta$ = 3.27–3.98 (m, 84H, H of C-3, C-5, C-6, C-2, C-4 of β-CD), 4.83 (d, $J$ = 4 Hz, 4H, $-CH_2-$), 4.89 (s, 4H, $-CH_2-$), 4.97–5.10 (m, 14H, H of C-1 of β-CD), 7.72–7.75 (m, 4H, H of phenanthroline and triazole), 8.10 (s, 2H, H of phenanthroline), 8.31 (d, $J$ = 8 Hz, 2H, H of phenanthroline); $^{13}$C NMR (100 MHz, $D_2O$, ppm): $\delta$ = 56.1, 64.2, 65.2, 68.4, 76.3, 76.7, 77.0, 78.0, 86.1, 88.0, 106.4, 106.8, 126.8, 131.3, 131.8, 132.9, 142.7, 148.5, 148.8, 162.3 ppm; MALDI-TOF MS: $m/z$: 2636.88 $[M + H]^+$, 2658.87 $[M + Na]^+$; elemental analysis calcd (%) for $C_{104}H_{154}N_8O_{70} \cdot 19H_2O$: C 41.94; H 6.50; N 3.76; found: C 41.85; H 6.40; N 4.10.

## Acknowledgements

We thank 973 Program (2011CB932502) and NNSFC (91227107, 21272125 and 21102075) for financial support.

## References

1 (*a*) T. Hirano, K. Kikuchi, Y. Urano, T. Higuchi and T. Nagano, *J. Am. Chem. Soc.*, 2000, **122**, 12399–12400; (*b*) Z. Xu, K.-H. Baek, H. N. Kim, J. Cui, X. Qian, D. R. Spring, I. Shin and J. Yoon, *J. Am. Chem. Soc.*, 2010, **132**, 601–610; (*c*) H. A. Godwin and J. M. Berg, *J. Am. Chem. Soc.*, 1996, **118**, 6514–6515; (*d*) N. C. Lim, H. C. Freake and C. Brückner, *Chem.–Eur. J.*, 2005, **11**, 38–49; (*e*) E. Kimura and S. Aoki, *BioMetals*, 2001, **14**, 191–204.

2 (*a*) C. J. Frederickson, J.-Y. Koh and A. I. Bush, *Nat. Rev. Neurosci.*, 2005, **6**, 449–462; (*b*) P. Jiang and Z. Guo, *Coord. Chem. Rev.*, 2004, **248**, 205–229; (*c*) Y.-H. Zhou, M. Zhao, Z.-W. Mao and L.-N. Ji, *Chem.–Eur. J.*, 2008, **14**, 7193–7201; (*d*) N. P. Pavletich and C. O. Pabo, *Science*, 1991, **252**, 809–817; (*e*) P. J. Fraker and L. E. King, *Annu. Rev. Nutr.*, 2004, **24**, 277–298; (*f*) S. Yamasaki, K. Sakata-Sogawa, A. Hasegawa, T. Suzuki, K. Kabu, E. Sato, T. Kurosaki, S. Yamashita, M. Tokunaga, K. Nishida and T. Hirano, *J. Cell Biol.*, 2007, **177**, 637–645; (*g*) T. V. O'Halloran, *Science*, 1993, **261**, 715–725.

3 (*a*) F. A. Cotton and G. Wilkinson, *Advanced Inorganic Chemistry*, John Wiley & Sons, New York, 4th edn, 1980; (*b*) M. Li, H.-Y. Lu, R.-L. Liu, J.-D. Chen and C.-F. Chen, *J. Org. Chem.*, 2012, **77**, 3670–3673.

4 (*a*) K. Komatsu, Y. Urano, H. Kojima and T. Nagano, *J. Am. Chem. Soc.*, 2007, **129**, 13447–13454; (*b*) F. Qian, C. Zhang, Y. Zhang, W. He, X. Gao, P. Hu and Z. Guo, *J. Am. Chem. Soc.*, 2009, **131**, 1460–1468; (*c*) S. Atilgan, T. Ozdemir and E. U. Akkaya, *Org. Lett.*, 2008, **10**, 4065–4067.

5 (*a*) J. Yuasa, A. Mitsui and T. Kawai, *Chem. Commun.*, 2011, **47**, 5807–5809; (*b*) Y. Zhang, X. Guo, W. Si, L. Jia and X. Qian, *Org. Lett.*, 2008, **10**, 473–476; (*c*) L. Xue, C. Liu and H. Jiang, *Org. Lett.*, 2009, **11**, 1655–1658.

6 (*a*) Y. Yang, Y.-M. Zhang, Y. Chen, D. Zhao, J.-T. Chen and Y. Liu, *Chem.–Eur. J.*, 2012, **18**, 4208–4215; (*b*) K. Uekama, F. Hirayama and T. Irie, *Chem. Rev.*, 1998, **98**, 2045–2076.

7 (*a*) Y. Liu, N. Zhang, Y. Chen and L.-H. Wang, *Org. Lett.*, 2007, **9**, 315–318; (*b*) Y. Liu, M. Yu, Y. Chen and N. Zhang, *Bioorg. Med. Chem.*, 2009, **17**, 3887–3891; (*c*) Y.-M. Zhang, Y. Chen, Z.-Q. Li, N. Li and Y. Liu, *Bioorg. Med. Chem.*, 2010, **18**, 1415–1420; (*d*) Y. Chen, Z.-H. Sun, B.-E. Song and Y. Liu, *Org. Biomol. Chem.*, 2011, **9**, 5530–5534; (*e*) B.-W. Liu, Y. Chen, B.-E. Song and Y. Liu, *Chem. Commun.*, 2011, **47**, 4418–4420.

8 T. Irie and K. Uekama, *Adv. Drug Delivery Rev.*, 1999, **36**, 101–123.

9 C. Hocquelet, J. Blu, C. K. Jankowski, S. Arseneau, D. Buisson and L. Mauclaire, *Tetrahedron*, 2006, **62**, 11963–11971.

10 (*a*) Y. Liu, Y. Song, Y. Chen, X.-Q. Li, F. Ding and R.-Q. Zhong, *Chem.–Eur. J.*, 2004, **10**, 3685–3696; (*b*) Y. Liu, H.-M. Yu, Y. Chen and Y.-L. Zhao, *Chem.–Eur. J.*, 2006, **12**, 3858–3868; (*c*) Y. Liu, J. Shi and D.-S. Guo, *J. Org. Chem.*, 2007, **72**, 8227–8234.

11 X.-L. Tang, X.-H. Peng, W. Dou, J. Mao, J.-R. Zheng, W.-W. Qin, W.-S. Liu, J. Chang and X.-J. Yao, *Org. Lett.*, 2008, **10**, 3653–3656.

12 M. Kajtár, C. Horvath-Toro, E. Kuthi and J. Szejtli, *Acta Chim. Acad. Sci. Hung.*, 1982, **110**, 327–355.

13 B. Balan and K. R. Gopidas, *Chem.–Eur. J.*, 2007, **13**, 5173–5185.

14 E. Bombarda, B. P. Roques, Y. Mély and E. Grell, *Biochemistry*, 2005, **44**, 7315–7325.

 